論文 Prediction of Stress-Strain Curve for Confined Concrete Based on Transverse Steel-Concrete Interaction

Minehiro NISHIYAMA[*1], Benny Beni ASSA[*2], Fumio WATANABE[*1]
and Naoki TAKAMORI[*3]

ABSTRACT: Constitutive relations for concrete under axial and lateral compressive stresses are derived based on experimental results of axial loading tests on confined and unconfined concrete cylinders. An analytical confinement model is applied to cross sections with various types of transverse reinforcement configuration. Stress and strain at peak load are evaluated by the constitutive relations obtained and lateral stress calculated. A procedure which can predict a whole stress - strain curve of confined concrete based on transverse reinforcement and concrete interaction is proposed. The theoretically obtained results are compared with experimental ones.
KEYWORDS: confined concrete, transverse reinforcement, stress - strain curve, lateral stress, lateral strain

1. INTRODUCTION

Various kinds of stress - strain curve models for concrete confined by transverse reinforcement have been proposed. Some of them focused on lateral expansion of concrete and reaction of transverse reinforcement to concrete. In this paper, a procedure which can predict a whole stress-strain curve for confined concrete using transverse steel - concrete interaction is proposed.

2. CONSTITUTIVE RELATIONS FOR CONCRETE

Uniaxial stress-strain relation of confined concrete can usually be formulated provided that at least three governing parameters are known; (1) initial tangential stiffness (2) stress and strain at peak axial load and (3) stress and strain of a point on the descending branch.

By studying in depth the test results of axial loading tests on the confined concrete cylinders reported in the reference [1], it is apparent that the attainable lateral pressure at maximum axial load is the key factor that determines the maximum stress and strain at peak axial load and the shape of the descending branch of the axial stress-strain curve. In order to derive a mathematical expression for the stress-strain relation, the stress-strain characteristics of confined concrete are related to the lateral pressure attained at maximum axial load.

2.1 LATERAL STRESS AND LATERAL STRAIN AT PEAK AXIAL LOAD

Based on the experimental results reported in the reference [1] the following expressions for the lateral stress and strain of confined concrete cylinders are derived.

$$\frac{f_{rp}}{f_{r,\max}} = \frac{8.0}{e^{(6.0\,s/D_c)}\, f_c'^{0.34}} \leq 1.0 \qquad (1)$$

*1 Department of Architectural Engineering, Kyoto University, DR, Member of JCI
*2 Department of Civil Engineering, Sam Ratulangi University, Indonesia
*3 Graduate student, Department of Architectural Engineering, Kyoto University, Member of JCI

in which f_{rp} is the lateral pressure at peak; $f_{r,\max}$ is the maximum potential lateral pressure, $f_{r,\max} = 2f_u A_s / sD_c$. f_u, A_s and s are the tensile strength, the sectional area and the spacing of the spiral, respectively; D_c is the diameter of confined concrete cylinder; e=2.718 (natural logarithmic number) and f_c' is concrete compressive strength in MPa. The ratio $f_{rp}/f_{r,\max}$ calculated by Eq. 1 is plotted in Fig. 1 against the one from the experiment.

$$\varepsilon_{rp} = 0.21 + 1.60\frac{f_{rp}}{f_c'} \qquad (2)$$

in which ε_{rp} is the lateral strain at peak of confined cylinder in %. Eq. 2 represents the locus of points having a pair of lateral stress and lateral strain values that determines the peak load condition for a given concrete strength. Fig. 2 shows the comparison of ε_{rp} estimated by Eq. 2 with the experimental results.

2.2 AXIAL STRESS AND AXIAL STRAIN AT PEAK LOAD

Fig. 3 shows the relations between the measured maximum stress and the corresponding lateral pressure reported in the reference[1]. Linear regression analysis of these data results in Eq. 3.

$$\frac{f_{cc}}{f_c'} = 1 + 3.36\frac{f_{rp}}{f_c'} \qquad (3)$$

in which f_{cc} is the maximum stress of confined concrete. The formula was derived based on the proposal by Richart et al.[2] The only difference is the coefficient of the second term of the right hand side.

The ratio of strain at peak load of confined concrete, ε_{cc}, to the strain at peak load of the plain cylinder, ε_{uc}, was determined by regression as shown in Fig. 3 and expressed by Eq. 4.

$$\frac{\varepsilon_{cc}}{\varepsilon_{uc}} = 1.0 + 21.5\frac{f_{rp}}{f_c'} \qquad (4)$$

2.3 STIFFNESS OF CONCRETE IN LATERAL DIRECTION

For a spirally confined concrete cylinder lat-

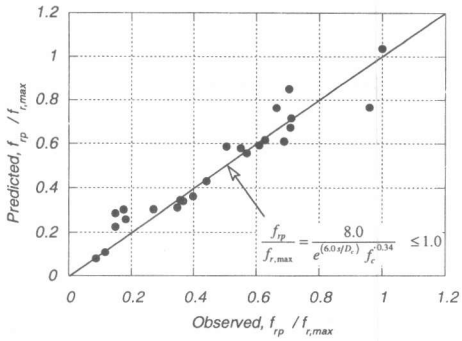

Fig. 1 Prediction of $f_{rp}/f_{r,\max}$

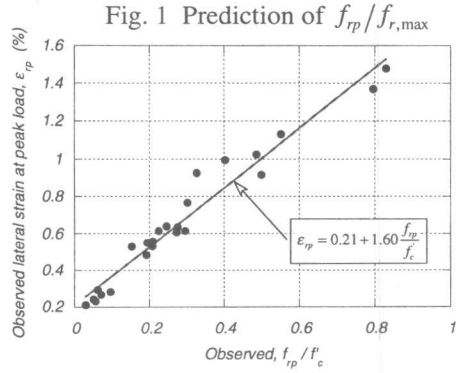

Fig. 2 Estimation of ε_{rp}

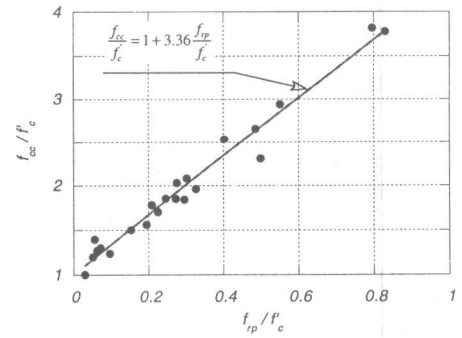

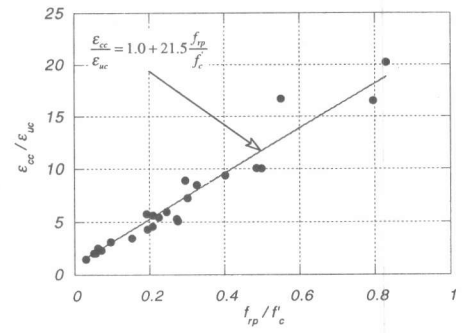

Fig. 3 f_{cc}/f'_c and $\varepsilon_{cc}/\varepsilon_{uc}$

eral strain can be expressed as

$$\varepsilon_r = \upsilon\,\varepsilon_c - \frac{f_r}{E_{cr}}(1-\upsilon) \tag{5}$$

in which υ is the Poisson's ratio as a function of axial stress-strain level; ε_c is the axial strain; E_{cr} is the tangential modulus of elasticity of concrete in the lateral direction as a function of lateral stress-strain level. If the first term of the right-hand side is known, the tangential stiffness E_{cr} is determined from the measured lateral stress and strain. Due to difficulties in measuring the lateral strains of plain concrete on the large deformation stage, the secant lateral stiffness up to $1/3 \cdot f_c'$ of concrete given in Eq. 6 is assumed in this study based on υ (=0.17) in the initial elastic range. In this study the stiffness of concrete element, E_{cr} is needed to determine the relative confining effect of various configuration of confining steel as shown later. Therefore, what is essential in the analysis in Section 3 is the relative stiffness between concrete elements. The error in determination of E_{cr} does not affect the evaluation of confining effect as long as the same E_{cr} is used in all concrete elements.

$$E_{cr} = \frac{100}{e^{3s/D_c}}\left(f_c'\right)^{1.2} \tag{6}$$

3. ANALYSIS OF TRANSVERSE REINFORCEMENT SYSTEM TO PREDICT LATERAL PRESSURE FOR VARIOUS TYPES OF CONFIGURATIONS

3.1 IDEALIZATION OF TRANSVERSE STEEL - CONCRETE INTERACTION

A reinforced concrete cross section with a peripheral hoop is shown in Fig. 6a. The concrete is discretized into a number of segments bounded by the steel bar element and the lines joining the centre point *O* and the midpoint between two nodes as shown in Fig. 6b. The lateral confining steel bars are also divided into a number of finite elements. The interaction of the concrete segments and the steel bar elements is idealized as shown in Fig. 7a. The concrete segment is represented by an axial compressive element having axial stiffness k_c and zero tension strength shown in Fig. 7b. The equilibrium and compatibility conditions between concrete and steel elements are enforced at all nodes.

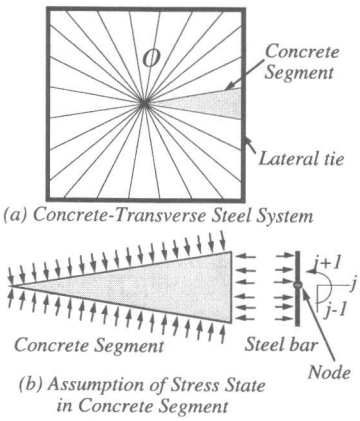

Fig. 6 Basic concept of confining mechanism

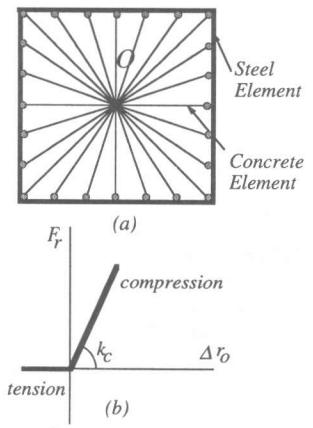

Fig. 7 Modeling of steel-concrete system

In this model, all concrete segments are subjected to uniform free lateral strain. Therefore, each concrete element pushes the lateral steel outwards at each node. The restraint action of the lateral steel depends on the axial compressive stiffness of the concrete element and the lateral stiffness and/or flexural stiffness of the steel system at each node.

3.2 STIFFNESS OF CONCRETE ELEMENT

An idealized axial concrete element is shown in Fig. 8. The lateral com-

pressive stress is assumed to be uniform along the steel element and along the boundary lines of the concrete segments. Nodal force F_r is given as

$$F_r = f_r L_e s \tag{7}$$

The axial compressive deformation of the segment, Δr_o is given by Eq. 8.

$$\Delta r_o = \int_0^{r_o} \varepsilon_r(r)\,dr = \frac{F_r r_o}{L_e s E_{cr}} \tag{8}$$

The stiffness of the concrete element k_c is defined as $F_r / \Delta r_o$. Therefore,

$$k_c = \frac{F_r}{\Delta r_o} = \frac{L_e s E_{cr}}{r_o} \tag{9}$$

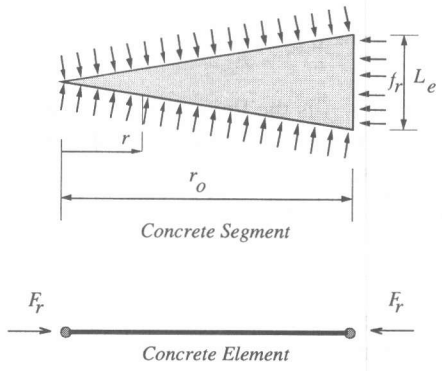

Fig. 8 Idealization of concrete element

3.3 FORMULATION OF STEEL FINITE ELEMENT

Fig. 9 shows a beam-column finite element with a number of monitoring sections. The reference system of coordinate for the element is the local coordinate system X, Y, which does not coincide with the global reference system. The longitudinal axis X is taken at the geometric centroid of the section shown in the figure. The load-deformation behavior of the element is determined by the behavior of the monitoring sections. Each section is discretized into fibres defined with respect to the member axis. The contribution of stress gradient within each layer to the bending moment is considered. Each fibre follows the uniaxial stress strain relations of reinforcing steel. The idealized stress-strain curve under monotonic loading derived by Yokoo and Nakamura [3] was used in this study.

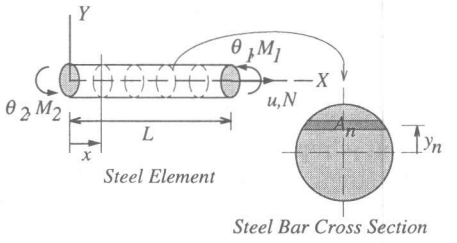

Fig. 9 Steel finite element

4. NUMERICAL EXAMPLES

Six configurations of transverse reinforcement shown in Fig. 10 were analyzed. The transverse steel with yield strength of 1300MPa and the concrete with compressive strength of 34.1 MPa were used for all types. The spacing of the transverse reinforcement was 70mm and therefore the volumetric ratio to the concrete core was 2.15%. The same volumetric ratio and spacing were assigned to all types although the bar diameters were different. The peripheral hoop is divided into 24 elements. The analysis was proceeded to obtain nodal force increment ΔF_r corresponding to the small increment of the lateral strain in the plain concrete. The lateral stress-lateral strain relations are plotted in Fig. 11a. The lateral stress and strain plotted in this figure are obtained by averaging the lateral stress and strain values at all nodes. The

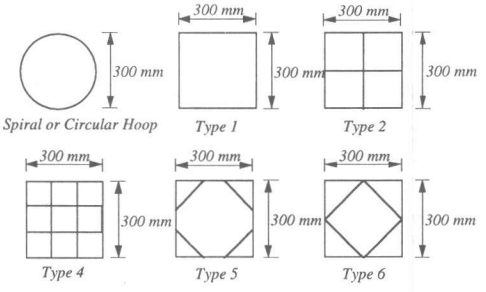

Fig. 10 Configurations of transverse steel

spiral is the most effective and the simple tie (Type 1) is the least. Fig. 11b shows an example of the distribution of lateral stresses along one side of the peripheral tie at the lateral strain of 3.0%. The lateral stress provided by the spiral is uniform, while the distribution of lateral stresses in the other configurations depends on the number of cross-ties.

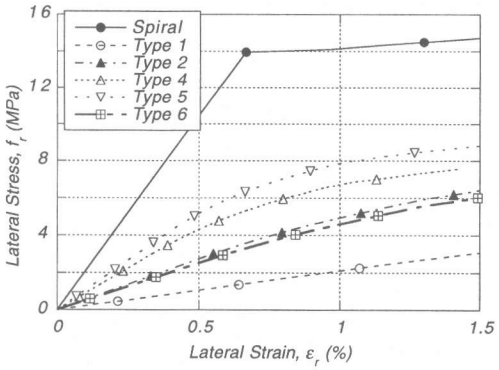

a) Average lateral stress-strain relations

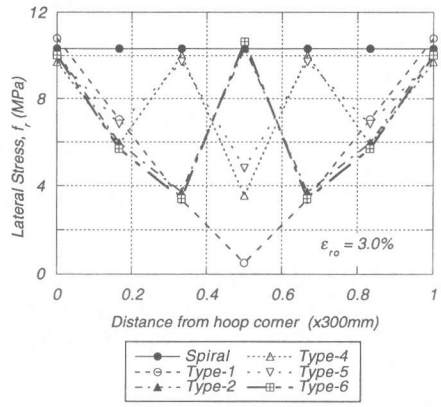

b) Distribution of lateral stress along one side of the peripheral hoop

Fig. 11 Theoretically predicted lateral stress for various types of configurations

5. DETERMINATION OF STRESS-STRAIN VALUES AT PEAK LOAD AND STRESS-STRAIN CURVE FOR CONFINED CONCRETE COLUMN

The relationship between the lateral strain and lateral stress at peak axial load can be expressed in Eq. 2. This equation gives the peak load condition of confined concrete, hence referring herein to Peak Load Condition of Confined concrete as PLCC line, that is a boundary between the pre-peak and post-peak state for a given concrete strength. If the observed lateral strain and stress coordinate is located above this line, the corresponding axial stress-strain point is located on the ascending branch of the stress-strain curve. If the observed lateral strain and stress coordinate is located below this line, the corresponding point is located on the descending branch.

On the other hand, the lateral stress-lateral strain relations of the transverse steel system obtained from the computer analysis depict the potential of the transverse reinforcement in providing the lateral pressure to concrete. By enforcing compatibility in the lateral deformation between concrete and the transverse steel system, the lateral stress and lateral strain at peak load may be determined from the intersection of the PLCC line and the lateral stress-lateral strain curve of the transverse steel system. In order to follow the form of PLCC line equation given by Eq. 2, the lateral stress is normalized by concrete cylinder strength f_c' as illustrated in Fig. 12. Having obtained the f_{rp}/f_c' value at the intersection, the lateral pressure f_{rp} at peak axial load can be calculated and the axial stress f_{cc} and strain ε_{cc} at peak may further be determined from Eqs. 3 and 4.

Twenty one column specimens were chosen for the comparison; one circular column labelled 30-M-25 in the reference [1] and twenty square columns tested by other researchers. The peak stress of the twenty square columns predicted using the proposed method

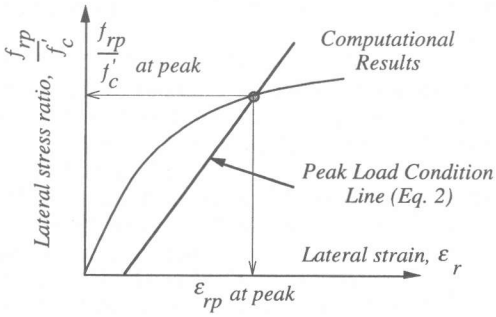

Fig. 12 Determination of lateral stress at peak load

are compared in Fig. 13 with the experimental results.

Fig. 14 shows one of the examples in which a stress-strain curve predicted by the above method is compared with the experimental results. To obtain a complete stress - strain curve the equations proposed by Popovics [3] was used. The figure indicated that the proposed method has capability of predicting the stress-strain curve of confined concrete with enough accuracy.

6. CONCLUSIONS

A prediction procedure of stress-strain curves of confined concrete based on lateral stress and strain was proposed. The predicted curves agreed well with the experimental results.

ACKNOWLEDGMENT

Mr. T. Kuroyama and Mr. T. Ikeuchi are appreciated for their help in performing the research.

REFERENCES

1. Takamori, T., Assa, B., Nishiyama, M. and Watanabe, F., "Idealization of Stress-Strain Relationship of Confined Concrete," Proc. of JCI, Vol.18, No.2, 1996, pp.395-400.
2. Richart, F. E. et al., "A Study of the Failure of Concrete under Combined Compressive Stresses", University of Illinois, Engineering Experimental Station, Bulletin No. 185, 1928.
3. Yokoo, Y. , and Nakamura, T. , "Non-stationary Hysteretic Uniaxial Stress-Strain Relations of Wide-Flange Steel : Part II - Empirical Formulae ", Transactions of Architectural Institute of Japan, No.260, Oct 1977, pp.143 - 149.
4. Popovics, S., "A numerical Approach to the Complete Stress-strain Curves of Concrete", Cement and Concrete Research, Vol.3, No.5, September 1973, pp.583-599.

References in Fig. 13;

Sheikh, S. A. and Uzumeri, S. M., "Strength and Ductility of Tied Concrete Columns", Journal of Structural Division, ASCE, Vol.106, No. ST5, May 1980, pp.1078-1102.

Scott, B. D., Park, R., and Priestley, M. J. N., "Stress-Strain Behavior of Concrete Confined by Overlapping Hoops at Low and High Strain Rates", ACI Journal, January-February 1982, Title No.79-2, pp.13-27.

Moehle, J. and Cavanagh, T., "Confinement Effectiveness of Crossties in RC", Journal of Structural Division, ASCE, Vol.111, No. ST10, October 1985.

Nishiyama, M. et al., "Axial Loading Tests on High-Strength Concrete Prisms Confined by Ordinary and High-Strength Steel", Proceedings of High-Strength Concrete 1993, Lillehammer Norway, pp.322-329.

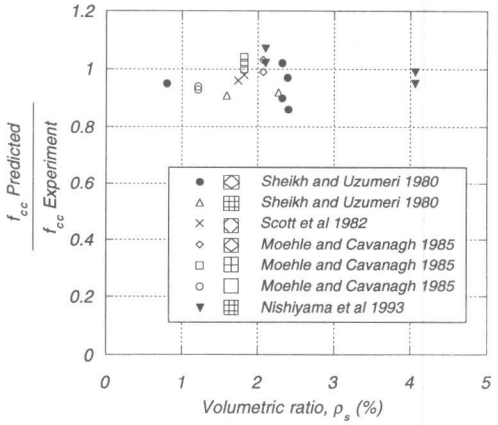

Fig. 13 Predicted strength - experimental results of various concentric load tests of RC columns

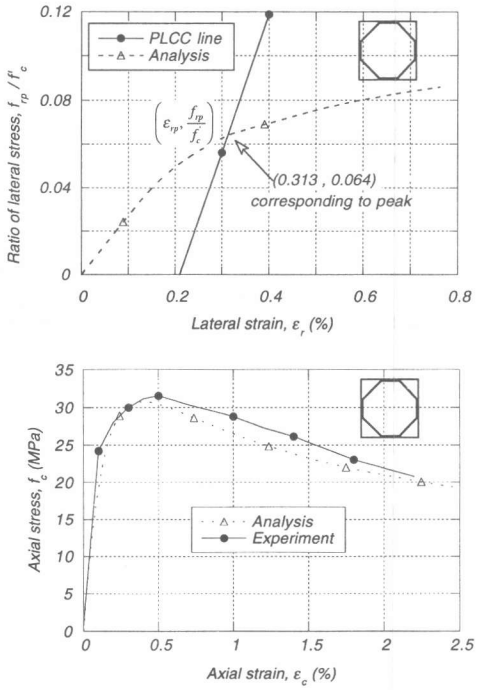

Fig. 14 Comparison between predicted and observed stress-strain curves of Unit-2 (Scott et al. 1982)